

Suppression of viscous fluid fingering: a piecewise constant-injection process

Eduardo O. Dias, Fernando Parisio, and José A. Miranda*

Departamento de Física, Universidade Federal de Pernambuco, Recife, PE 50670-901 Brazil

The injection of a fluid into another of larger viscosity in a Hele-Shaw cell usually results in the formation of highly branched patterns. Despite the richness of these structures, in many practical situations such convoluted shapes are quite undesirable. In this letter we propose an efficient and easily reproducible way to restrain these instabilities based on a simple piecewise constant pumping protocol. It results in a reduction in the size of the viscous fingers by one order of magnitude.

PACS numbers: 47.15.gp, 47.20.Hw, 47.54.-r, 47.55.N-

Hydrodynamic fingering is one of a wider class of interfacial instabilities occurring when one material is injected into another, or grows from a given chemical, biological or geophysical process. Examples of such pattern forming systems include the classic Saffman-Taylor (ST) instability [1], the dynamics of chemically reacting fronts [2], the growth of filamentary organisms [3], and lava flows [4]. These seemingly unrelated processes produce complex patterns presenting similar morphological features, where highly branched shapes and dendriticlike configurations may arise. In this context, the control of the growth and form of the emerging complex morphologies has long been a challenging topic, of great academic and technological relevance.

Due to its relative simplicity, and multiple applications the ST instability has received much attention, and serves as a paradigm for pattern formation systems [5]. This instability arises when a fluid is injected against a second of much larger viscosity in the narrow gap between closely-spaced parallel glass plates of a Hele-Shaw (HS) cell [6]. Under constant flow injection rate, the result is the development of vastly ramified interfacial patterns [7–11]. One of the most important practical situations related to this hydrodynamic instability is oil recovery [12], where petroleum is displaced by injection of water into the oil field in an attempt to extract more oil from the well. Interestingly, the dynamic behavior for flow in HS cells is described by the very same set of equations as those for flow in porous media [5]. In fact, the ST instability is a major source of poor oil recovery, once rapidly evolving fingers may reach the entrance of the well, and mainly water, and not oil is retrieved. This emblematic example clearly illustrates the importance of developing a fundamental understanding of the dynamics of this type of system, and to find ways to contain, and possibly suppress such interfacial disturbances.

Very recently, some research groups [13–15] have examined the possibility of avoiding the emergence of the usual branched morphology, by properly controlling the flow injection rate. Instead of considering a constant injection flux, they assumed a particular time-varying pumping rate which scaled with time like $C(n)t^{-1/3}$, where $C(n)$ depends on the interfacial wave number n .

Their theoretical and experimental findings demonstrate that by using this specific pumping rate the formation of branched patterns is inhibited, and replaced by n -fold symmetric shapes. This process conveniently determines the number of emerging fingers. In spite of this controlling strategy, the resulting interfacial morphologies are notably noncircular, and still contain sizable fingers. Therefore, the interfacial fingering perturbations are not exactly wiped out, but redesigned into self-similar shapes with a prescribed number of fingers. In this sense, an efficient protocol for suppressing the development of the viscous fingering instability in radial HS flows is still lacking.

Differently to what is done in Refs. [13–15], we consider a simple piecewise constant injection process which results in the actual suppression of the viscous fingering instability. In the usual constant injection situation, a certain amount of fluid is pumped in a finite time, and interfacial fingering results. In the procedure we suggest the average injection rate is kept unchanged, so that the same amount of fluid is injected in the same time interval, but interfacial irregularities are restrained.

We begin by briefly describing the traditional radial flow setup in confined geometry. Consider a HS cell of gap spacing b containing two immiscible, incompressible, viscous fluids. The viscosities of the fluids are denoted as η_1 and η_2 , and between them there exists a surface tension σ . Fluid 1 is injected into fluid 2 at a constant injection rate Q_0 , equal to the area covered per unit time. Linear stability analysis of the problem [7–9] considers harmonic distortions of a nearly circular fluid-fluid interface whose radius evolves according to $\mathcal{R}(\theta, t) = R(t) + \zeta_n(t) \cos n\theta$, where the time dependent unperturbed radius is $R(t) = R_t = \sqrt{R_0^2 + Q_0 t/\pi}$, θ represents the azimuthal angle, and $n=0, \pm 1, \pm 2, \dots$ are discrete wave numbers. The unperturbed radius of the interface at $t = 0$ is represented by R_0 , and the Fourier perturbation amplitudes are given by

$$\zeta_n(t) = \zeta_n(0) \exp\{I_0(n)\}, \quad I_0(n) = \int_0^t \lambda(n) dt' \quad (1)$$

where the linear growth rate is

$$\lambda(n) = \left[f(n) \frac{Q_0}{R^2} - g(n) \frac{1}{R^3} \right], \quad (2)$$

with $f(n) = (A|n| - 1)/2\pi$, $g(n) = [b^2\sigma|n|(n^2 - 1)]/[12(\eta_1 + \eta_2)]$, and $A = (\eta_2 - \eta_1)/(\eta_2 + \eta_1)$ being the viscosity contrast. If $I_0(n) > 0$ the disturbance grows, indicating instability. In Eq. (2) we notice opposing effects of the viscosity difference between the fluids (destabilizing) and of the surface tension (stabilizing). A relevant information can be extracted at the linear stage: the existence of a series of critical radii $R_c(n)$ [or critical times $t_c(n)$] at which the interface becomes unstable for a given mode n [defined by setting $\lambda(n) = 0$], characterizing a cascade of modes [9]. Therefore, to write the linear solution in a more realistic way, one should consider the interval $[t_c(n), t_f]$ only, because integration over $[0, t_c(n)]$ would lead to an artificial diminishing in the size of the fingers, so that $\zeta_n(t_c(n)) < \zeta_n(0)$. This is an unphysical effect because we assume that the amplitudes can not go below $\zeta_n(0)$ due to noncontrollable factors, e.g., irregularities on the surface of the plates [8]. For this reason we will consider the initial perturbation to be independent of n , that is, $\zeta_n(0) \equiv \zeta_0$. Notice, however, that for lower modes $t_c(n) \ll t_f$, and solution (1) can be used as a good approximation.

We proceed by describing the stabilization protocol. Consider a radial HS flow, and suppose that one is required to pump a fluid into the cell, at a specified average rate Q_0 , during the time interval $[0, t_f]$. This defines the final area occupied by the injected fluid, $\mathcal{A}_f = \pi R_0^2 + Q_0 t_f$. Given the quantities \mathcal{A}_f and t_f , our goal is to design a simple injection process that suppresses viscous fingering events occurring at usual constant pumping procedure which utilizes the same input parameters \mathcal{A}_f and t_f . The results presented here refer to $\mathcal{A}_f \approx 140 \text{ cm}^2$ and $t_f = 28.0 \text{ s}$ ($Q_0 = 5.00 \text{ cm}^2/\text{s}$) and to the following set of characteristic physical parameters: $R_0 = 0.30 \text{ cm}$, $b = 0.10 \text{ cm}$, $\zeta_0 = R_0/2400 \approx 10^{-4} \text{ cm}$, $\sigma = 63.0 \text{ dyne/cm}$, $\eta_2 = 5.21 \text{ g/cm s}$, and $\eta_1 \approx 0$. These values are consistent with those used in typical experimental realizations [7–11]. We chose $A \approx 1$ because in this limit the most *unstable* situation is reached, so that the results can only improve for $0 < A < 1$.

Out of a plethora of possibilities for time-varying injection scenarios, the simplest nontrivial procedure is a two-stage piecewise constant pumping (Fig. 1), whose choice will be justified shortly. Specifically, we split the time interval $[0, t_f]$ into $[0, \tau]$, during which the constant injection rate is Q ; and $[\tau, t_f]$, with $t_f = (1 + \beta)\tau$, for which the injection is given by γQ . The requirement that the average injection remains unchanged demands that

$$Q = \frac{(1 + \beta)}{(1 + \gamma\beta)} Q_0, \quad (3)$$

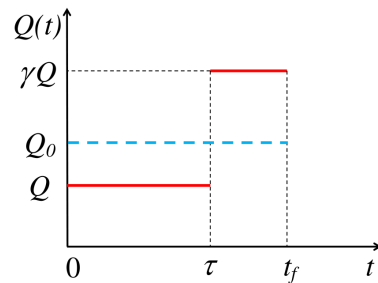


FIG. 1. (Color online) Injection rate $Q(t)$ as a function of time for a two-stage piecewise constant protocol. The equivalent constant injection rate Q_0 is represented by the horizontal dashed line.

with $\beta > 0$ and $\gamma\beta > -1$. If the parameter γ is negative we have an injection stage followed by a period of suction. For $\gamma > 0$ two nontrivial possibilities arise: if $\gamma < 1$ the injection in the first stage is stronger than in the second, and for $\gamma > 1$ the weaker injection stage comes first. For $\gamma = 1$ we recover the usual constant pumping situation.

As commented earlier, the formal output of a linear analysis is given by Eq. (1) for the constant injection, while for the lower modes in the two-stage pumping we have $\zeta'_n(t) = \zeta_0 \exp\{I'(n)\}$ with

$$I'(n) = \int_0^\tau \lambda_1(n) dt + \int_\tau^{t_f} \lambda_2(n) dt = 2\pi f(n) \Lambda(R_f, R_0) - \frac{2\pi g(n)(1 + \beta\gamma)}{Q_0(1 + \beta)} \left[\frac{1}{\gamma} \Gamma(R_f, R_\tau) + \Gamma(R_\tau, R_0) \right] \quad (4)$$

where λ_1 and λ_2 refer to the first and second stages with their respective injection rates, $\Lambda(x, y) = \ln(x/y)$, and $\Gamma(x, y) = (1/y - 1/x)$. Note that while R_0 and R_f , the initial and final unperturbed radii, are constant, the radius at $t = \tau$, is a function of the free parameters, $R_\tau = R_\tau(\beta, \gamma)$.

If we are to suppress instabilities, at least for the initial modes, we must impose that $\zeta'_n/\zeta_n = \exp\{I' - I_0\} < 1$ in the end of the whole process, i.e., at $t = t_f$. By analyzing the overall sign in the argument of the exponential one shows that the only scenario that leads to stabilization is that with $\gamma > 1$, or, an initial stage with a relatively weak injection rate followed by a stronger (by a factor of γ) injection stage. This can be understood by recalling that the lower the mode the larger its maximum growth rate. So, to suppress the initial and larger instabilities a slow injection is needed. For the other scenarios no values of β and γ produce a stabilizing effect. We have also checked oscillating pumping with $Q(t) > 0$ and oscillations involving injection and suction in each cycle, both resulting in an enhancement of the ST instability. Thus, our task is to establish a general and simple way to obtain optimal values, β^* and γ^* , within the selected scenario ($\beta > 0$ and $\gamma > 1$).

It is a key point to realize that during the piece-

wise constant injection the cascade of modes occurs differently. In general, the “wakening” of lower modes still occurs in the first stage of pumping. However, for $t = t_f/(1 + \beta) = \tau$ the injection rate jumps discontinuously and two effects occur: the most unstable modes prior to the sudden change in the pumping regime have their growth rates drastically decreased, and, at the same time, a certain number of new modes become unstable instantaneously. After that the cascade process continues. We have used a smoothed out version of the step-like injection function depicted in Fig. 1 and verified that the outcome is virtually unchanged. This signifies that our results are not due to any peculiarity related to the discontinuous nature of $Q(t)$.

In our quest for the optimal parameters β^* and γ^* , we try to devise simple rules that are *independent* of the discrete wave number. For this reason, we will suppose that the relevant modes approximately fit in one out of two classes: (i) modes that become unstable soon after the beginning of the first stage (lower modes), and (ii) modes which attain their regimes of instability exactly at $t = \tau$ or a bit later (higher modes). The remaining modes, i.e., those which become unstable at the end of first stage [$t \sim t_f/(1 + \beta)$] and in the final part of the second stage ($t \sim t_f$) are not critical because their regime of strong instability lasts for a short time. The effectiveness of these considerations will be made evident in what follows. For

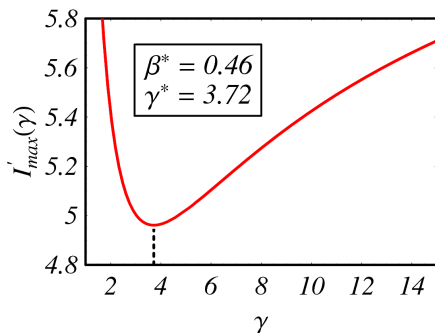


FIG. 2. (Color online) Behavior of $I'_{max} = I''_{max}$ as a function of γ . The absolute minimum at $\gamma^* = 3.72$ is indicated.

the relevant modes of type (i) we have the perturbations appropriately described by Eq. (4), while for the modes of type (ii) we have $\zeta''_m(t) = \zeta_0 \exp\{I''(m)\}$, where

$$I''(m) = \int_{\tau}^{t_f} \lambda_2(m) dt = 2\pi f(m) \Lambda(R_f, R_0) - \frac{2\pi g(m)(1 + \beta\gamma)}{\gamma Q_0(1 + \beta)} \Gamma(R_f, R_{\tau}). \quad (5)$$

In order to get rid of the dependence on n and m , we will focus on the modes associated to the largest perturbation amplitudes in each stage, n_{max} and m_{max} , respectively. Therefore, we can guarantee that the size of the fingers corresponding to these wave numbers constitute an upper

bound for the scale of all other modes. This is obtained by setting $\partial I'/\partial n = 0$ and $\partial I''/\partial m = 0$, yielding

$$n_{max} = \sqrt{\frac{1}{3} + \frac{2Q_0(\eta_1 + \eta_2)\gamma(1 + \beta)\Lambda(R_f, R_0)}{\pi b^2 \sigma(1 + \beta\gamma) [\Gamma(R_f, R_{\tau}) + \gamma\Gamma(R_{\tau}, R_0)]}}, \quad (6)$$

and

$$m_{max} = \sqrt{\frac{1}{3} + \frac{2Q_0(\eta_1 + \eta_2)\gamma(1 + \beta)\Lambda(R_f, R_{\tau})}{\pi b^2 \sigma(1 + \beta\gamma)\Gamma(R_f, R_{\tau})}}. \quad (7)$$

The referred upper bounds are then $I'(n_{max})$ and

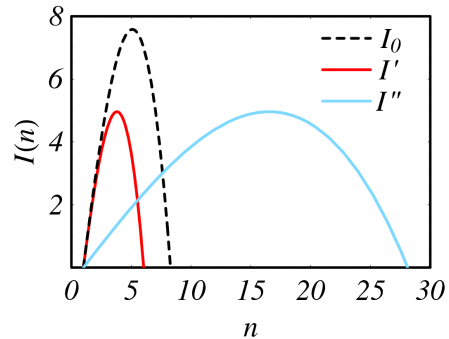


FIG. 3. (Color online) The continuous curves represent I' and I'' as functions of n , calculated for β^* and γ^* . The dashed curve shows the corresponding quantity I_0 for the constant injection process.

$I''(m_{max})$. Before imposing any minimization condition on these quantities we make sure that the suppression of the instabilities is uniform, with higher modes as controlled as the lower ones, by setting the constraint

$$I'(n_{max}) = I''(m_{max}) \Rightarrow I'_{max}(\beta, \gamma) = I''_{max}(\beta, \gamma), \quad (8)$$

which reduces the dimension of our space of parameters and can be numerically solved to give $\beta(\gamma)$. Using this relation to eliminate β in $I'_{max}(\beta, \gamma)$, or $I''_{max}(\beta, \gamma)$, we obtain a function of the single variable γ , shown in Fig. 2. Finally, we pick the value of this variable that minimizes I'_{max} [and automatically I''_{max} due to (8)], that corresponds to the optimal value $\gamma^* = 3.72$ and also yields $\beta^* = \beta(\gamma^*) = 0.46$. This completely characterizes the piecewise constant injection and gives $\tau \approx 19.2$ s before which the injection rate is $Q = 2.7$ cm²/s, with the stronger pumping lasting for about 8.8 s with an injection of $\gamma Q = 10$ cm²/s. In Fig. 3 we show $I'(n)$, $I''(n)$ (optimal parameters used), and I_0 for the equivalent constant pumping process as functions of the wave number. Condition (8) is evident from this figure and, most importantly, we have $I_{0max} \approx 7.5$ and $I'_{max} = I''_{max} \approx 4.9$. Since these integrals are related to the logarithm of the amplitude, the decrease in the relative size of the largest fingers is of one order of magnitude. The effectiveness of the protocol can be seen even more clearly in Fig. 4,

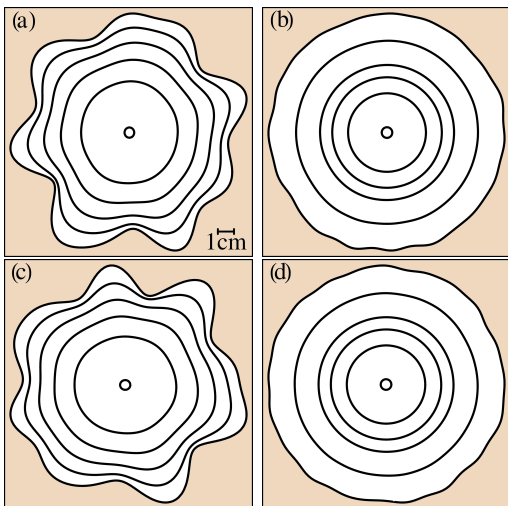


FIG. 4. (Color online) Comparison between the interfacial patterns formed during constant injection (a), and piecewise constant injection (b) including 40 Fourier modes and a random choice of phases. The same is valid for figures (c) and (d), respectively, but considering 30 modes, and a different set of random phases.

where we plot the linear evolution of the interfaces for the equivalent constant pumping in (a) and (c), and for the two-stage pumping in (b) and (d). The patterns on the top have the same initial conditions (including the random phases attributed to each mode [8, 9]), and 40 Fourier modes have been considered. The same is valid for the two bottom panels, but including 30 modes and a distinct set of random phases. The interfaces are plotted in intervals of $t_f/5$. Note that they are spaced in a more uniform way for the constant injection, while for the piecewise constant injection the interfaces are initially closely spaced, and then more widely separated. We emphasize that the cascade of modes was considered without any simplifying hypothesis in these numerical results. Moreover, notice that the shapes shown in Fig. 4(b) and Fig. 4(d) are very similar, revealing an insensitivity to changes in the initial conditions.

We have also investigated the weakly nonlinear evolution of the interfaces by considering both second and third order couplings [9], and verified that our protocol produces patterns nearly identical to those depicted in Fig. 4(b) and Fig. 4(d). This indicates that the emer-

gence of nonlinearities is unfavored, expanding the duration of the linear regime. However, the robustness of this stabilization for fully nonlinear stages of the dynamics merits further numerical and experimental investigation.

In conclusion, we have introduced a simple injection process for which interfacial viscous fingering instabilities are truly suppressed. The procedure does not rely on unusual material properties of fluids, or on drastic modifications of the traditional radial HS flow setup. It only requires the employment of an optimal two stage piecewise constant injection mechanism. This stabilization strategy might be useful to improve the efficiency and control of a number of physical, biological, and technological problems related to viscous fingering phenomena.

Financial support from CNPq, FACEPE, and FAPESQ (Brazilian agencies) is gratefully acknowledged.

* jme@df.ufpe.br

- [1] P. G. Saffman and G. I. Taylor, Proc. R. Soc. London Ser. A **245**, 312 (1958).
- [2] A. De Wit, Phys. Rev. Lett. **87**, 054502 (2001).
- [3] A. Goriely and M. Tabor, Phys. Rev. Lett. **90**, 108101 (2003).
- [4] R. W. Griffiths, Annu. Rev. Fluid Mech. **32**, 477 (2000).
- [5] K. V. McCloud and J. V. Maher, Phys. Rep. **260**, 139 (1995); J. Casademunt, Chaos **14**, 809 (2004).
- [6] H. S. Hele-Shaw, Nature (London) **58**, 34 (1898).
- [7] L. Paterson, J. Fluid Mech. **113**, 513 (1981).
- [8] M. J. P. Gingras and Z. Rácz, Phys. Rev. A **40**, 5960 (1989).
- [9] J. A. Miranda and M. Widom, Physica D **120**, 315 (1998).
- [10] O. Praud and H. L. Swinney, Phys. Rev. E **72**, 011406 (2005).
- [11] S. W. Li, J. S. Lowengrub, and P. H. Leo, J. Comput. Phys. **225**, 554 (2007).
- [12] S. B. Gorell and G. M. Homsy, SIAM J. Appl. Math. **43**, 79 (1983).
- [13] S. W. Li, J. S. Lowengrub, J. Fontana, and P. Palffy-Muhoray, Phys. Rev. Lett. **102**, 174501 (2009).
- [14] A. Leshchiner, M. Thrasher, M. B. Mineev-Weinstein, and H. L. Swinney, Phys. Rev. E **81** 016206 (2010).
- [15] E. O. Dias and J. A. Miranda, Phys. Rev. E **81**, 016312 (2010).